PNAS

Supporting Information for

Structure-guided approach to modulate small molecule binding to a promiscuous ligand-activated protein

Wenwei Lin[1,*], Andrew D. Huber[1,*,†], Shyaron Poudel[1], Yongtao Li[1], Jayaraman Seetharaman[2], Darcie J. Miller[2], Taosheng Chen[1,†]

This PDF file includes:

Supporting Text
Tables S1 to S4
Figures S1 to S24
SI References

SUPPORTING TEXT

Synthesis. Organic reagents were purchased from commercial suppliers unless otherwise noted and were used without further purification. All solvents were analytical or reagent grade and the solvents were dried using the Glass Contour Solvent Systems by SG Water USA. All reactions with water- and/or air-sensitive starting materials were carried out in pre-dried glass wares under argon atmosphere with standard procedure. Flash column chromatography was performed by using Biotage Isolera™ Flash Systems and Biotage® SNAP Ultra or Biotage® SNAP Ultra C18 columns (Biotage, Charlotte, NC). All reactions as well as compound purity were monitored by UPLC-MS by using a Waters Acquity UPLC MS system with a C18 column in a 2-min gradient (H_2O + 0.1% formic acid → acetonitrile + 0.1% formic acid) and detectors of PDA (215–400 nm), ELSD, and Acquity SQD ESI-positive MS (Waters Corporation, Milford, MA). High-resolution mass spectra were determined by using a Waters Acquity UPLC system with a C18 column (H_2O + 0.1% formic acid → acetonitrile + 0.1% formic acid gradient over 2.5 min) and Xevo G2Q-TOF ESI-positive MS in resolution mode. Compounds were internally normalized to leucine-enkephalin lock solution, with a calculated error of <3 ppm. All final compounds used for SAR studies have purity at 95% or greater. All NMR spectra were recorded on a Bruker 500 MHz spectrometer (Bruker Corporation) in the solvents indicated and spectra were processed using MestReNova (14.1.0) (Mestrelab Research). The chemical shift values are expressed in parts per million (ppm) relative to tetramethylsilane as the internal standard. Coupling constants (*J*) are reported in hertz (Hz). **T0-C4**, **T0-C5**, **T0-C6**, **T0-C8**, and **T0-BP** are also known as **SJPYT-302**, **SJPYT-315**, **SJPYT-316**, **SJPYT-317** and **SJPYT-319**, respectively; this nomenclature is used in the following methods.

Synthesis of the analogs (**SJPYT-302**, **315-317** and **319**) is described in Figure S5 under the conditions described by B. P. Fauber et al. (1). Treatment of 2-(4-Aminophenyl)-1,1,1,3,3,3-hexafluoropropan-2-ol (**1a**) with benzenesulfonyl chloride in the presence of 2,6-Lutidine gave N-[4-(1,1,1,3,3,3-Hexafluoro-2-hydroxypropan-2-yl)phenyl]benzenesulfonamide (**1b**). The secondary aniline (**1b**) was then alkylated with respective alkyl-halides in the presence of potassium carbonate and heating to produce the target N-alkyl analogs **SJPYT-302**, **315-317** and **319**.

***N*-(4-(1,1,1,3,3,3-hexafluoro-2-hydroxypropan-2-yl)phenyl)benzenesulfonamide (1b).** To a solution of 2-(4-aminophenyl)-1,1,1,3,3,3-hexafluoropropan-2-ol (1a, 5g, 19.29 mmol) in acetone (30 mL) at room temperature, benzenesulfonyl chloride (2.59 ml, 20.26 mmol) and 2,6-dimethylpyridine (4.13 g, 38.6 mmol) was added. The mixture was allowed to stir at 60 ºC for overnight. After the complete consumption of the substituted aniline, the reaction mixture was concentrated, and water (100 mL) was added. The aqueous layer was extracted with EtOAc (100 mL × 2). The combined organic layer was washed with brine. The organic layer was then dried over $MgSO_4$, filtered, and concentrated under reduced pressure. The obtained residue was purified by silica gel chromatography (0% to 100% acetonitrel in water) to give *N*-(4-(1,1,1,3,3,3-hexafluoro-2-hydroxypropan-2-yl)phenyl)benzenesulfonamide (1b, 6.78 g, 88% yield) as an off-white solid. ^{1}H NMR (500 MHz, DMSO-d_6) δ 11.21 (s, 1H), 9.10 (s, 1H), 8.45 – 8.24 (m, 2H), 8.18 – 8.12 (m, 1H), 8.11 – 8.00 (m, 4H), 7.81 – 7.67 (m, 2H).

***N*-butyl-*N*-(4-(1,1,1,3,3,3-hexafluoro-2-hydroxypropan-2-yl)phenyl)benzenesulfonamide (SJPYT-302, T0-C4).** A solution of *N*-(4-(1,1,1,3,3,3-hexafluoro-2-hydroxypropan-2-yl)phenyl)benzenesulfonamide (1b, 200 mg, 0.501 mmol) in CH_3CN 5 mL at rt was mixed with K_2CO_3 (138 mg, 1.002 mmol)) and 1-iodobutane (62.7 µl, 0.551 mmol). The suspension was stirred at 70 ℃ for overnight. The reaction mixture was then added to water (50 mL) and extracted with EtOAc (50 mL × 2). The EtOAc layer was washed with water, dried with anhydrous Na_2SO_4, and concentrated under reduced pressure. The residue was purified by silica gel chromatography (0% to 100% EA in hexane) to give the product **SJPYT-302** (155.2 mg, 68% yield, 96.78% purity) as a white solid. ^{1}H NMR (500 MHz, DMSO-d_6) δ 8.80 (s, 1H), 7.74 – 7.68 (m, 1H), 7.66 (d, *J* = 8.4 Hz, 2H), 7.62 – 7.53 (m, 4H), 7.29 – 7.22 (m, 2H), 3.70 – 3.41 (m, 2H), 1.53 – 1.09 (m, 4H), 0.84 – 0.76 (m, 3H). ^{13}C NMR (126 MHz, DMSO-d_6) δ 140.83, 138.05, 133.73, 130.29, 129.82, 128.68, 128.07, 127.58, 126.73, 124.43, 122.14, 119.84, 77.38, 77.15, 76.91, 76.68, 49.60, 30.15, 19.31, 13.80. ESI-TOF HRMS: m/z 456.1081 ($C_{19}H_{19}F_6NO_3S$ + H^+ requires 456.1063).

***N*-(4-(1,1,1,3,3,3-hexafluoro-2-hydroxypropan-2-yl)phenyl)-*N*-pentylbenzenesulfonamide (SJPYT-315, T0-C5).** The title compound was synthesized using a similar procedure as described for **SJPYT-302** by employing **1b** and 1-iodopentane to give a white solid (199.7 mg, 85% yield, 100% purity). ^{1}H NMR (500

MHz, DMSO-d_6) δ 8.80 (s, 1H), 7.74 – 7.64 (m, 3H), 7.62 – 7.55 (m, 4H), 7.29 – 7.22 (m, 2H), 3.56 (t, *J* = 6.8 Hz, 2H), 1.37 – 1.14 (m, 6H), 0.77 (t, *J* = 6.9 Hz, 3H). ^{13}C NMR (126 MHz, DMSO-d_6) δ 139.78, 137.03, 132.66, 129.23, 128.76, 127.63, 127.00, 126.52, 125.67, 123.37, 121.08, 118.78, 76.55, 76.32, 76.09, 75.85, 75.62, 48.82, 30.10, 27.18, 26.64, 20.85, 13.14. ESI-TOF HRMS: m/z 470.1233 ($C_{20}H_{21}F_6NO_3S$ + H^+ requires 470.1219).

***N*-(4-(1,1,1,3,3,3-hexafluoro-2-hydroxypropan-2-yl)phenyl)-*N*-hexylbenzenesulfonamide (SJPYT-316, T0-C6).** The title compound was synthesized using a similar procedure as described for **SJPYT-302** by employing **1b** and 1-bromohexane to give a white solid (171.9 mg, 71% yield, 97.63% purity). ^{1}H NMR (500 MHz, DMSO-d_6) δ 8.80 (s, 1H), 7.74 – 7.62 (m, 3H), 7.61 – 7.53 (m, 4H), 7.28 – 7.23 (m, 2H), 3.56 (t, *J* = 6.7 Hz, 2H), 1.34 – 1.09 (m, 8H), 0.79 (t, *J* = 6.9 Hz, 3H). ^{13}C NMR (126 MHz, DMSO-d_6) δ 139.80, 137.04, 132.66, 129.23, 128.76, 127.63, 127.00, 126.53, 125.68, 123.38, 121.09, 118.79, 76.56, 76.33, 76.10, 75.86, 75.63, 48.83, 30.10, 29.93, 26.95, 24.64, 21.30, 13.16. ESI-TOF HRMS: m/z 484.1387 ($C_{21}H_{23}F_6NO_3S$ + H^+ requires 484.1376).

***N*-(4-(1,1,1,3,3,3-hexafluoro-2-hydroxypropan-2-yl)phenyl)-*N*-octylbenzenesulfonamide (SJPYT-317, T0-C8).** The title compound was synthesized using a similar procedure as described for **SJPYT-302** by employing **1b** and 1-iodooctane to give a white solid (63.4 mg, 64% yield, 99.05% purity). ^{1}H NMR (500 MHz, DMSO-d_6) δ 8.80 (s, 1H), 7.73 – 7.62 (m, 3H), 7.62 – 7.53 (m, 4H), 7.28 – 7.22 (m, 2H), 3.56 (t, *J* = 6.7 Hz, 2H), 1.32 – 1.12 (m, 12H), 0.82 (t, *J* = 7.1 Hz, 3H). ^{13}C NMR (126 MHz, DMSO-d_6) δ 139.79, 137.04, 132.66, 129.23, 128.76, 127.62, 127.00, 126.54, 125.68, 123.39, 121.09, 118.79, 76.56, 76.33, 76.09, 75.86, 75.63, 48.82, 30.49, 27.86, 27.65, 26.93, 24.95, 21.43, 13.29. ESI-TOF HRMS: m/z 512.1705 ($C_{23}H_{27}F_6NO_3S$ + H^+ requires 512.1689).

***N*-([1,1'-biphenyl]-4-ylmethyl)-*N*-(4-(1,1,1,3,3,3-hexafluoro-2-hydroxypropan-2-yl)phenyl)benzenesulfonamide (SJPYT-319, T0-BP).** The title compound was synthesized using a similar procedure as described for **SJPYT-302** by employing **1b** and 4-(bromomethyl)-1,1'-biphenyl to give a white solid (228.5 mg, 81% yield, 99.5% purity). ^{1}H NMR (500 MHz, DMSO-d_6) δ 8.74 (s, 1H), 7.79 – 7.71 (m, 1H), 7.70 – 7.54 (m, 10H), 7.43 (dd, *J* = 8.4, 7.1 Hz, 2H), 7.39 – 7.28 (m, 5H), 4.91 (s, 2H). ^{13}C NMR (126 MHz, DMSO-d_6) δ 139.84, 138.92, 138.67, 137.08, 134.74, 132.89, 129.01, 128.90, 128.31, 127.82, 127.30, 126.88, 126.86, 126.61, 126.07, 125.96, 125.59, 123.30, 121.00, 118.71, 76.47, 76.24, 76.01, 75.77, 75.54, 52.15. ESI-TOF HRMS: m/z 564.1082 ($C_{28}H_{21}F_6NO_3S$ - H^+ requires 564.1074).

Number	PDB ID	PubMed ID	Release Date	Ligand(s)
1	1ILG	11408620	6/27/2001	No Ligand
2	1ILH	11408620	6/27/2001	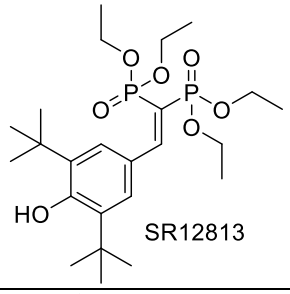 SR12813
3	1M13	12578355	3/4/2003	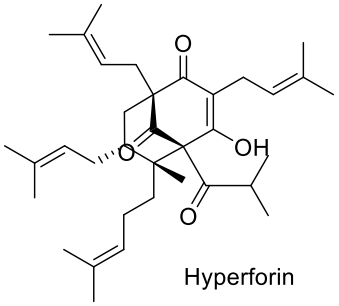 Hyperforin
4	1NRL	12909012	8/19/2003	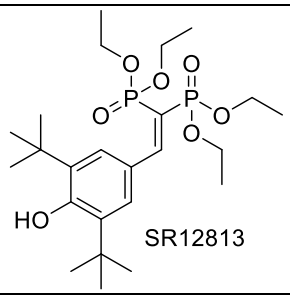 SR12813
5	1SKX	15705662	3/8/2005	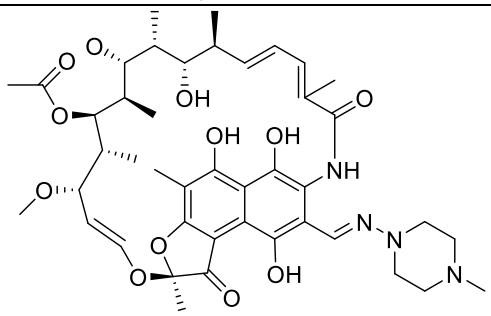 Rifampicin
6	2O9I	17215127	1/30/2007	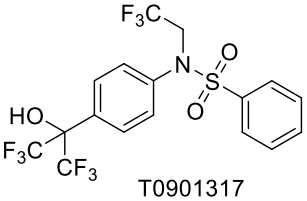 T0901317

7	2QNV	18768384	7/29/2008	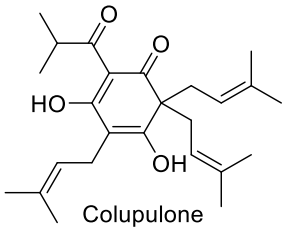 Colupulone
8	3CTB	18456871	12/2/2008	No Ligand
9	3HVL	18456871	8/4/2009	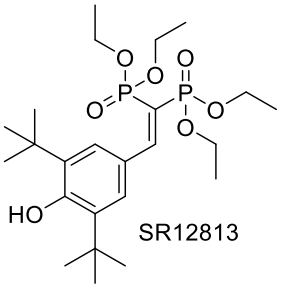 SR12813
10	3R8D	21805522	8/17/2011	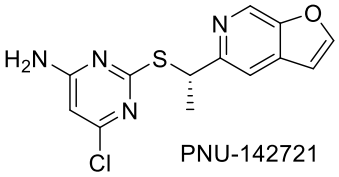 PNU-142721
11	4J5W	23602807	8/21/2013	No Ligand
12	4J5X	23602807	8/21/2013	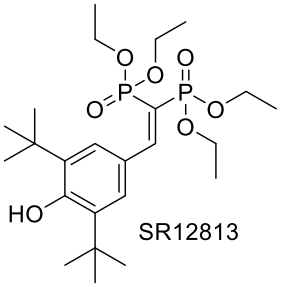 SR12813
13	4NY9	25101488	8/27/2014	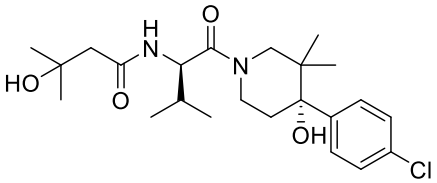 N-{(2R)-1-[(4S)-4-(4-chlorophenyl)-4-hydroxy-3,3-dimethylpiperidin-1-yl]-3-methyl-1-oxobutan-2-yl}-3-hydroxy-3-methylbutanamide
14	4XHD	25579995	1/28/2015	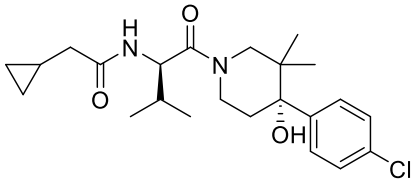 N-{(2R)-1-[(4S)-4-(4-chlorophenyl)-4-hydroxy-3,3-dimethylpiperidin-1-yl]-3-methyl-1-oxobutan-2-yl}-2-cyclopropylacetamide

15	4S0T	25579995	2/4/2015	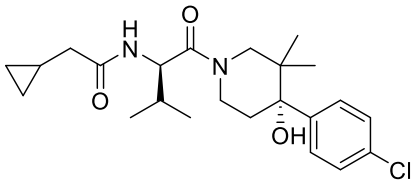 N-{(2R)-1-[(4S)-4-(4-chlorophenyl)-4-hydroxy-3,3-dimethylpiperidin-1-yl]-3-methyl-1-oxobutan-2-yl}-2-cyclopropylacetamide
16	4S0S	25579995	2/11/2015	No Ligand
17	4X1F	26333997	9/9/2015	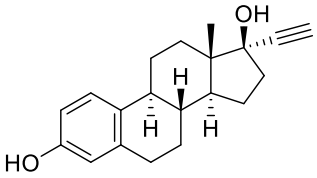 17α-ethinylestradiol
18	4X1G	26333997	9/9/2015	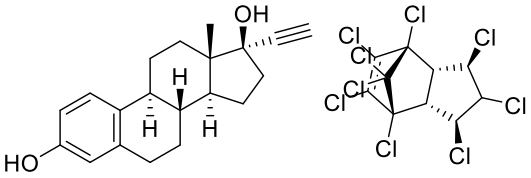 17α-ethinylestradiol *trans*-nonachlor
19	4XAO	26333997	9/9/2015	No Ligand
20	5A86	26291341	10/21/2015	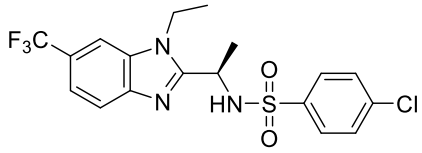 4-chloro-N-[(1R)-1-[1-ethyl-6-(trifluoromethyl)benzimidazol-2-yl]ethyl]benzenesulfonamide
21	5X0R	28963450	10/4/2017	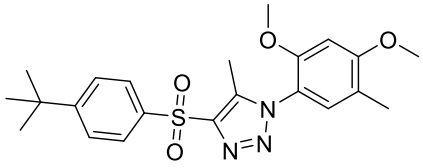 SJB7
22	6BNS	29233651	12/20/2017	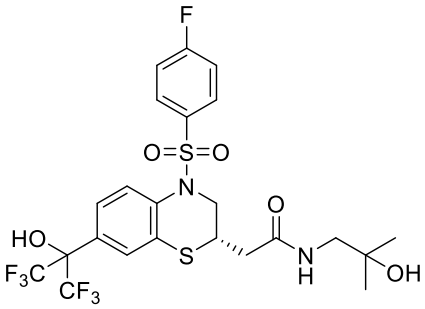 2-[(2S)-4-[(4-fluorophenyl)sulfonyl]-7-(1,1,1,3,3,3-hexafluoro-2-hydroxypropan-2-yl)-3,4-dihydro-2H-1,4-benzothiazin-2-yl]-N-(2-hydroxy-2-methylpropyl)acetamide

23	6DUP	30146095	8/29/2018	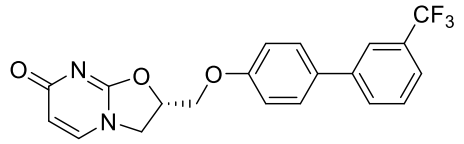 (2S)-2-({[3'-(trifluoromethyl)[1,1'-biphenyl]-4-yl]oxy}methyl)-2,3-dihydro-7H-[1,3]oxazolo[3,2-a]pyrimidin-7-one
24	6S41	31525968	10/2/2019	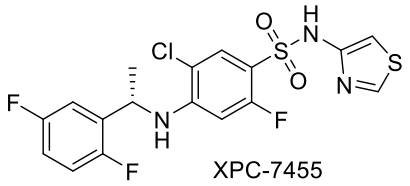 XPC-7455
25	6HTY	31746599	12/4/2019	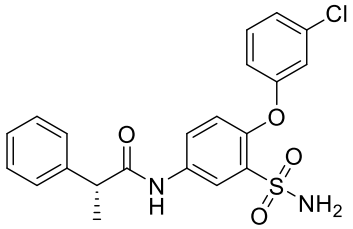 (2~{R})-~{N}-[4-(3-chloranylphenoxy)-3-sulfamoyl-phenyl]-2-phenyl-propanamide
26	6NX1	30891142	2/12/2020	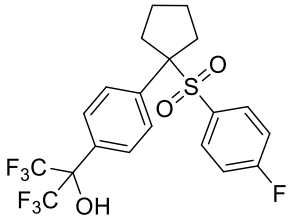 1,1,1,3,3,3-hexafluoro-2-(4-{1-[(4-fluorophenyl)sulfonyl]cyclopentyl}phenyl)propan-2-ol
27	6HJ2	34958586	3/25/2020	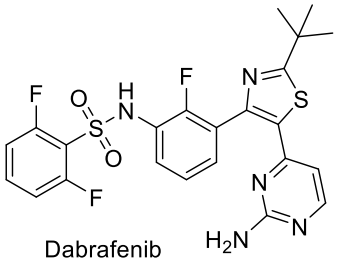 Dabrafenib
28	6P2B	32160459	4/1/2020	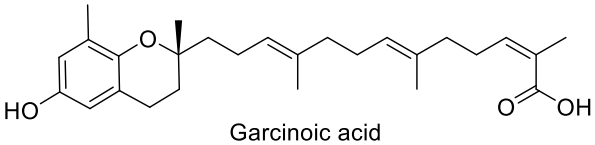 Garcinoic acid

29	6XP9	32890685	9/23/2020	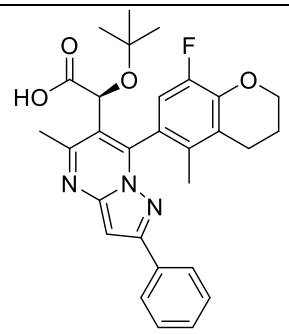 (2S)-tert-butoxy[7-(8-fluoro-5-methyl-3,4-dihydro-2H-1-benzopyran-6-yl)-5-methyl-2-phenylpyrazolo[1,5-a]pyrimidin-6-yl]acetic acid
30	6TFI	33108181	11/11/2020	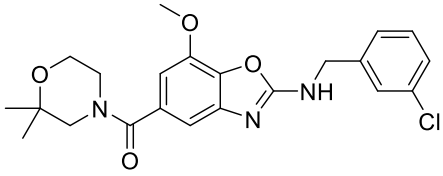 [2-[(3-chlorophenyl)methylamino]-7-methoxy-1,3-benzoxazol-5-yl]-(2,2-dimethylmorpholin-4-yl)methanone
31	7AX8	33361153	1/13/2021	No Ligand
32	7AX9	33361153	1/13/2021	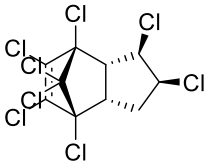 *cis*-chlordane
33	7AXA	33361153	1/13/2021	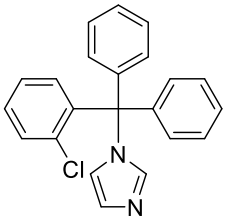 Clotrimazole
34	7AXB	33361153	1/13/2021	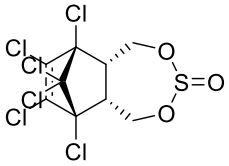 Endosulfan
35	7AXC	33361153	1/13/2021	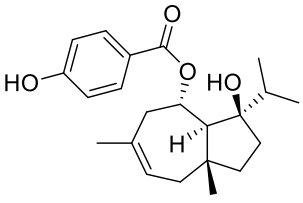 Ferutinine

36	7AXD	33361153	1/13/2021	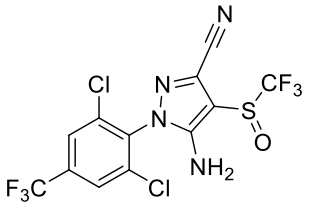 Fipronil
37	7AXE	33361153	1/13/2021	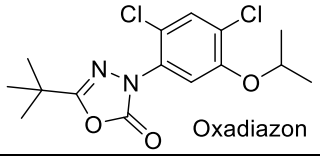 Oxadiazon
38	7AXF	33361153	1/13/2021	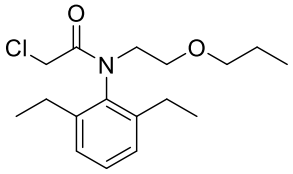 Pretilachlor
39	7AXG	33361153	1/13/2021	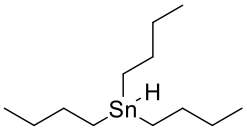 Tributyltin
40	7AXH	33361153	1/13/2021	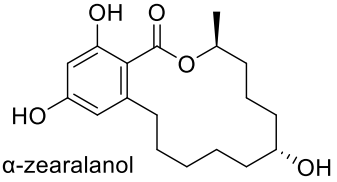 α-zearalanol
41	7AXI	33361153	1/13/2021	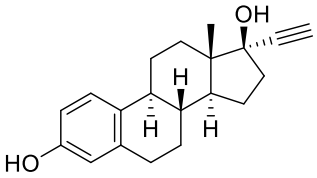 17α-ethinylestradiol 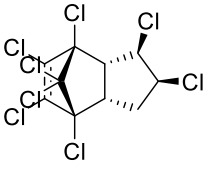 *cis*-chlordane
42	7AXJ	33361153	1/13/2021	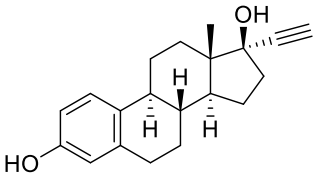 17α-ethinylestradiol 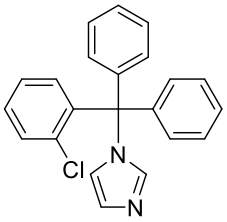 Clotrimazole
43	7AXK	33361153	1/13/2021	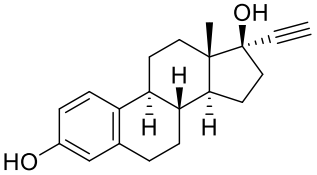 17α-ethinylestradiol 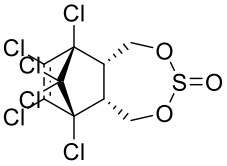 Endosulfan

44	7AXL	33361153	1/13/2021	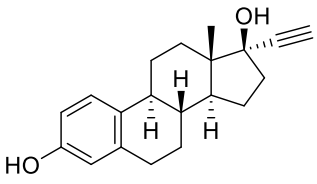 17α-ethinylestradiol 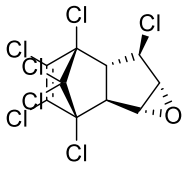 Heptachlor endo-epoxide
45	7CHG		7/7/2021	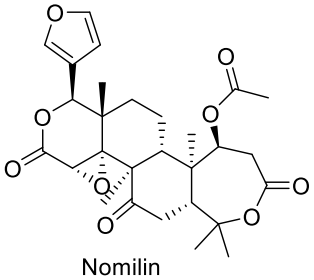 Nomilin
46	7N2A	34531948	8/25/2021	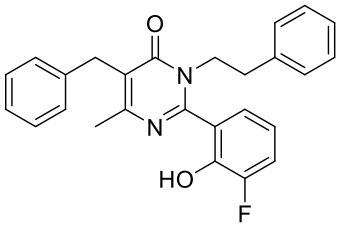 5-benzyl-2-(3-fluoro-2-hydroxyphenyl)-6-methyl-3-(2-phenylethyl)pyrimidin-4(3H)-one
47	7RIO	34531948	8/25/2021	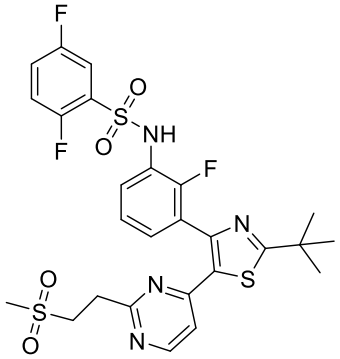 N-[3-(2-tert-butyl-5-{2-[2-(methanesulfonyl)ethyl] pyrimidin-4-yl}-1,3-thiazol-4-yl)-2-fluorophenyl]-2,5-difluorobenzene-1-sulfonamide
48	7RIU	34531948	8/25/2021	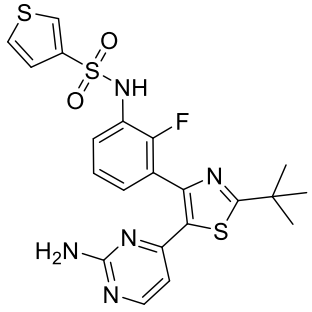 N-{3-[5-(2-aminopyrimidin-4-yl)-2-tert-butyl-1,3-thiazol-4-yl]-2-fluorophenyl}thiophene-3-sulfonamide

49	7RIV	34531948	8/25/2021	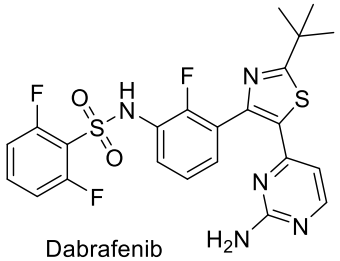 Dabrafenib

Table S1. List of PXR LBD structures deposited in the PDB.

Data Collection		
Resolution range (Å)		32.49-2.25 (2.37-2.25)
Space group		$P\ 4_3\ 2_1\ 2$
Unit cell dimensions		
	a, b, c (Å)	91.89, 91.89, 85.99
	α, β, γ (°)	90.0, 90.0, 90.0
Wavelength (Å)		0.97934
Unique reflections		18018
Redundancy		15.9 (11.2)
Completeness (%)		100.0 (100.0)
I/σI		21.6 (1.5)
R_{sym}		0.091 (0.784)
$CC_{1/2}$		1.000 (0.895)
Model Refinement		
R_{work}/R_{free}		0.208/0.235
Number of atoms		
	Protein	2196
	Ligand	50
	Water	111
RMSD		
	Bond length (Å)	0.005
	Bond angles (°)	0.8
Ramachandran plot (%)		
	Preferred	98.15
	Outliers	0.37
Clash score[a]		0.68
MolProbity score[a]		0.72
Average B-factor (Å^2)		49.0

Table S2. Data collection and model refinement statistics for the rifamycin S-bound PXR LBD structure (PDB code 8E3N). Values from the highest resolution shell are shown in parentheses. [a]Generated with MolProbity.

Data Collection		
Resolution range (Å)		36.76-2.30 (2.38-2.30)
Space group		*P* 4_3 2_1 2
Unit cell dimensions		
	a, b, c (Å)	91.10, 91.10, 85.21
	α, β, γ (°)	90.0, 90.0, 90.0
Wavelength (Å)		0.9201
Unique reflections		16633
Redundancy		14.7 (15.2)
Completeness (%)		99.9 (99.7)
I/σI		14.7 (2.3)
R_{sym}		0.114 (1.300)
$CC_{1/2}$		0.999 (0.815)
Model Refinement		
R_{work}/R_{free}		0.217/0.239
Number of atoms		
	Protein	2141
	Ligand	39
	Water	33
RMSD		
	Bond length (Å)	0.006
	Bond angles (°)	0.938
Ramachandran plot (%)		
	Preferred	97.79
	Outliers	0.00
Clash score[a]		0.94
MolProbity score[a]		1.03
Average B-factor (Å^2)		55.0

Table S3. Data collection and model refinement statistics for the T0-BP-bound PXR LBD structure (PDB code 8FPE). Values from the highest resolution shell are shown in parentheses. [a]Generated with MolProbity.

Data Collection		
Resolution range (Å)		29.67-2.37 (2.43-2.37)
Space group		*P* 2_1 2_1 2_1
Unit cell dimensions		
	a, b, c (Å)	85.37, 89.00, 105.57
	α, β, γ (°)	90.0, 90.0, 90.0
Wavelength (Å)		0.9201
Unique reflections		33262
Redundancy		6.8 (6.5)
Completeness (%)		99.4 (93.1)
I/σI		13.4 (2.1)
R_{sym}		0.081 (0.758)
$CC_{1/2}$		0.998 (0.749)
Model Refinement		
R_{work}/R_{free}		0.204/0.228
Number of atoms		
	Protein	4773
	Ligand	64
	Water	68
RMSD		
	Bond length (Å)	0.009
	Bond angles (°)	1.158
Ramachandran plot (%)		
	Preferred	96.14
	Outliers	0.18
Clash score[a]		0.87
MolProbity score[a]		1.42
Average B-factor (Å^2)		60.0

Table S4. Data collection and model refinement statistics for the T0-C6-bound PXR LBD-SRC-1 structure (PDB code 8EQZ). Values from the highest resolution shell are shown in parentheses. [a]Generated with MolProbity.

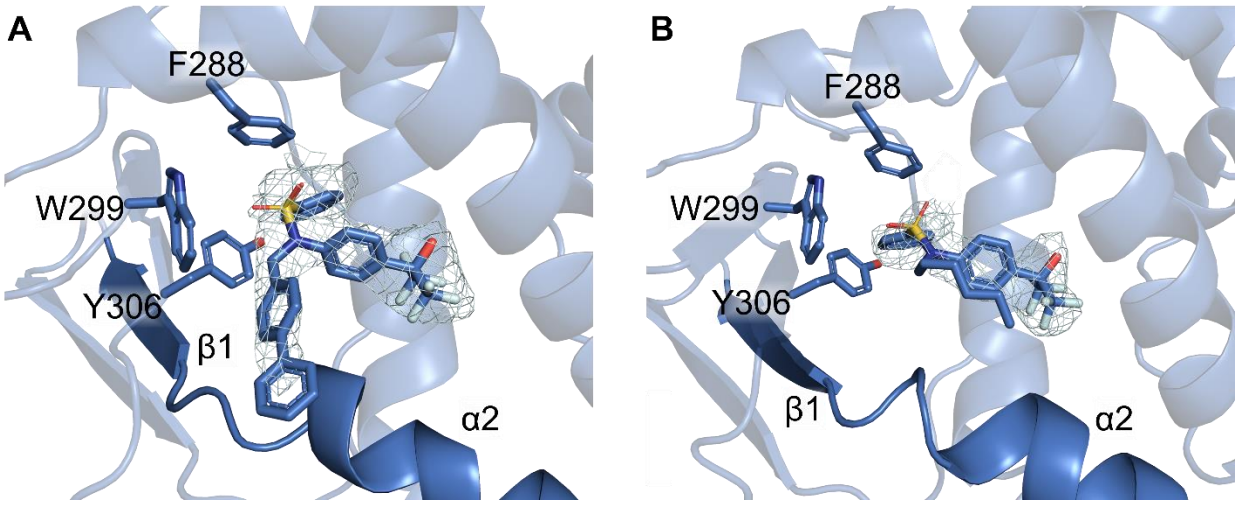

Figure S1. Electron density for (A) T0-BP and (B) T0-C6 in the PXR LBD. The 2Fo–Fc maps are contoured in mesh at 1.0 standard deviations and carved around ligands at 2 Å.

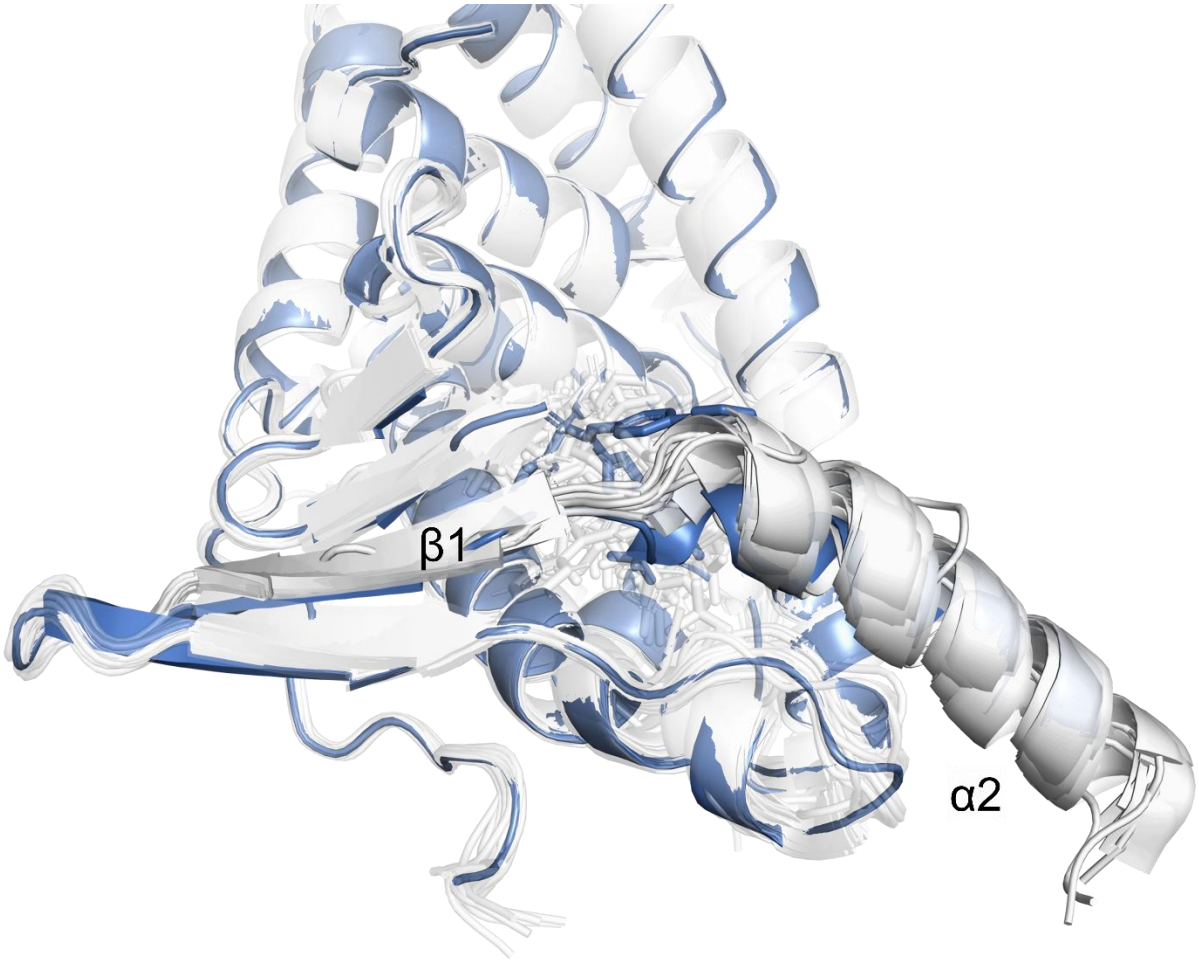

Figure S2. T0-BP significantly displaces α2-β1. All previously reported PXR LBD structures are overlaid with the T0-BP-bound structure colored in marine. Ligands are shown as sticks, and protein is represented as cartoon. The T0-BP structure overlays well with all other PXR LBD structures, but there is clear displacement of α2 and β1.

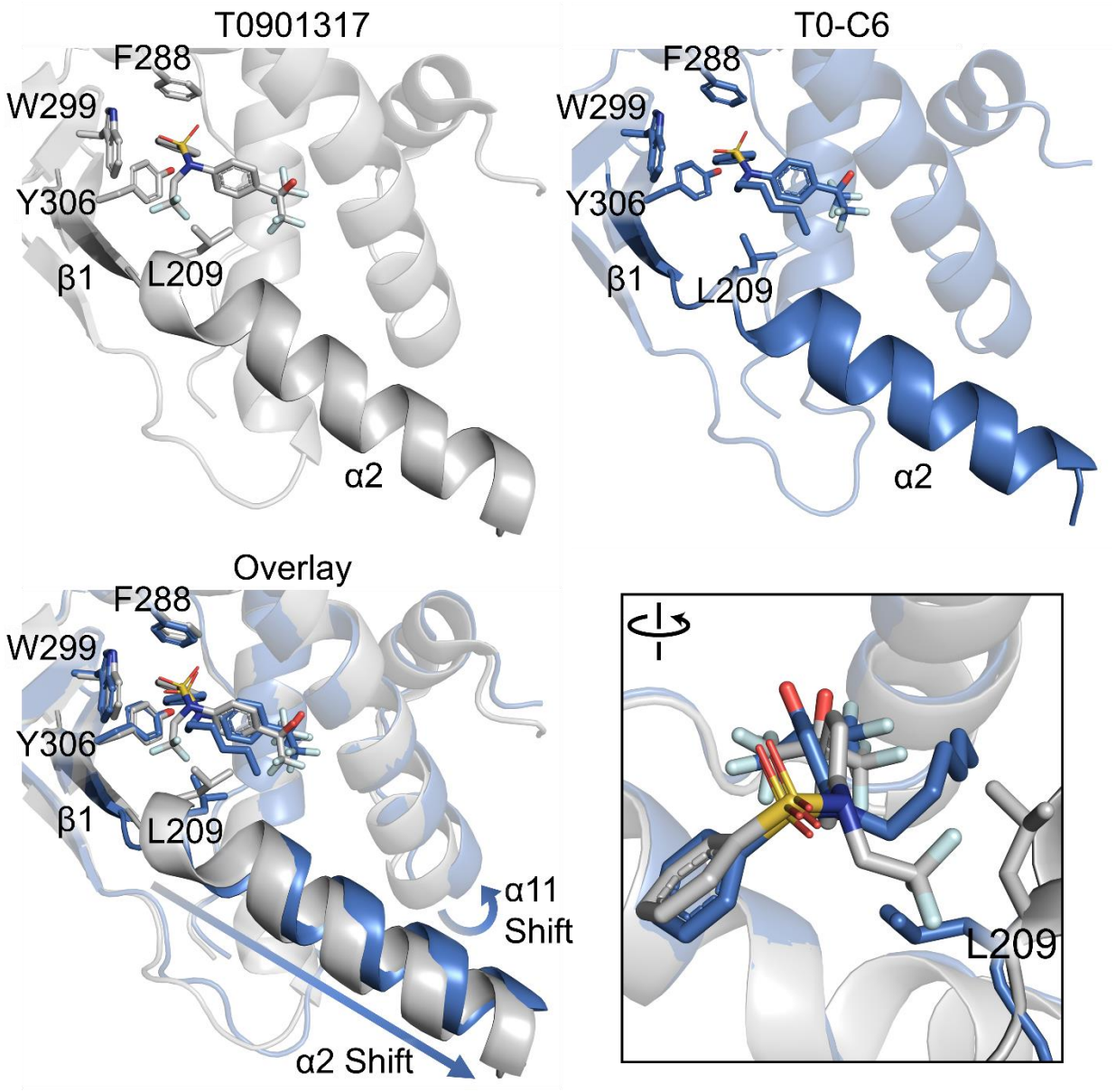

Figure S3. Comparison of T0901317-bound (PDB ID 2O9I, chain A) and T0-C6-bound PXR LBD (chain A). Panel 3 (Overlay) indicates the shifted α2 and α11, and panel 4 (highlighted with a box) is zoomed in to show the L209 flip.

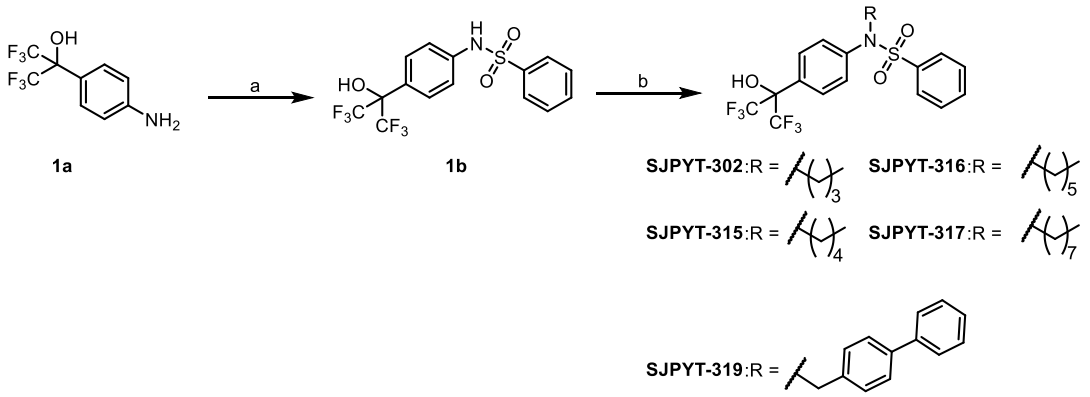

Figure S4. Synthesis of SJPYT-302, SJPYT-315, SJPYT-316, SJPYT-317 and SJPYT-319. Reagents and conditions: (a) Benzenesulfonyl chloride, 2,6-lutidine, acetone, reflux; (b) BrR or IR, K_2CO_3, CH_3CN, 70°C.

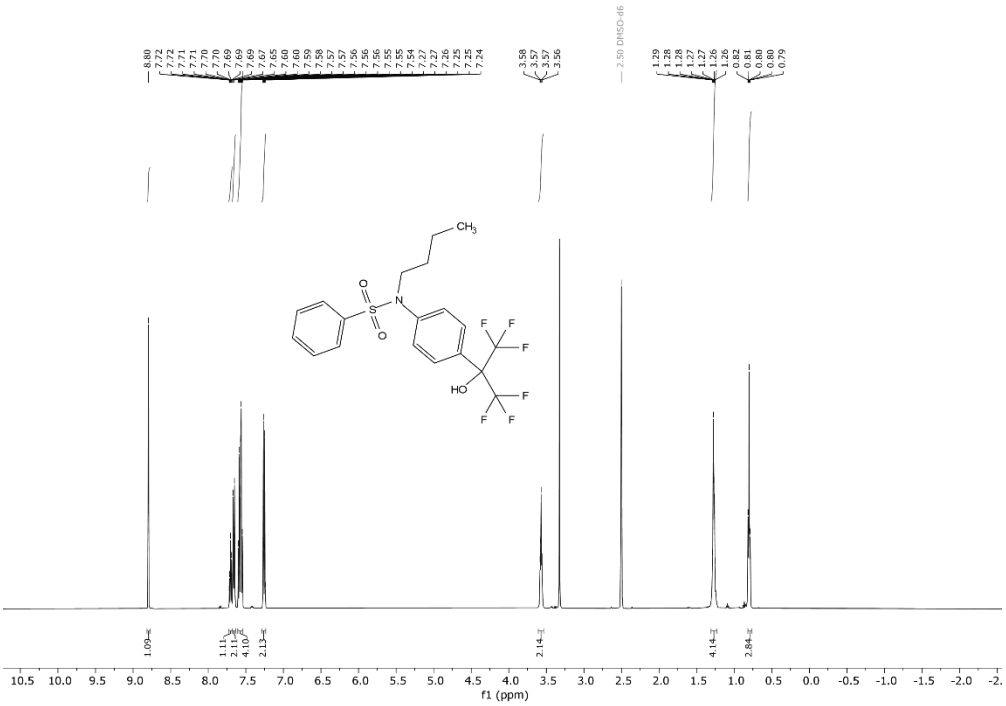

Figure S5. ^{1}H NMR of SJPYT-302.

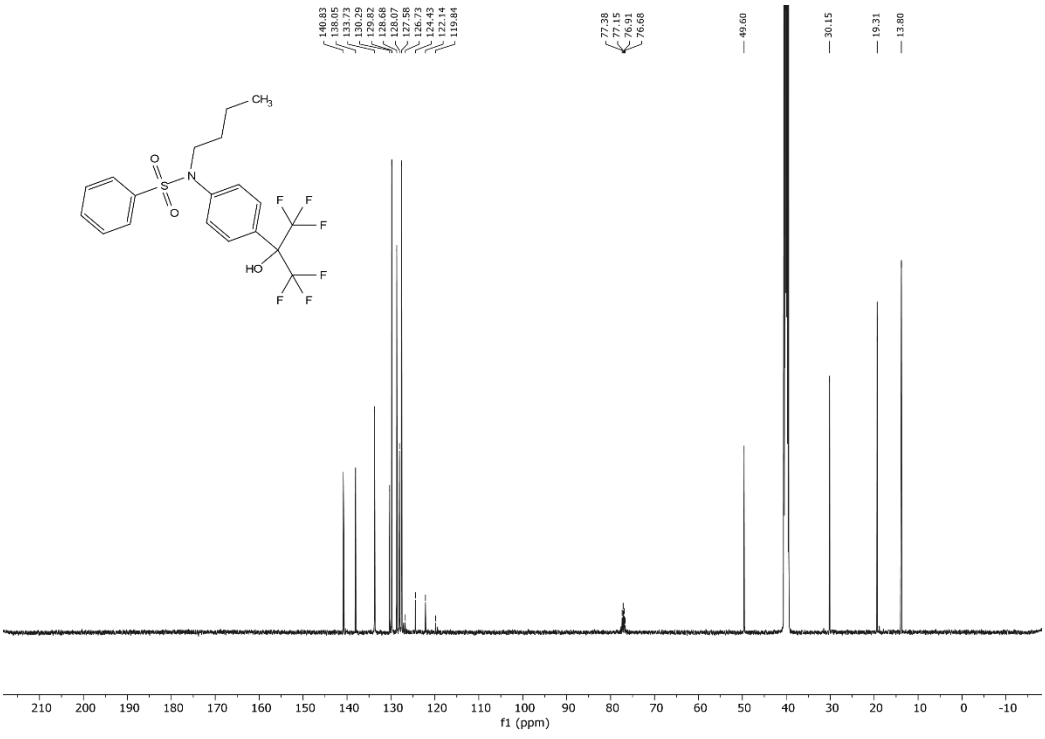

Figure S6. ^{13}C NMR of SJPYT-302.

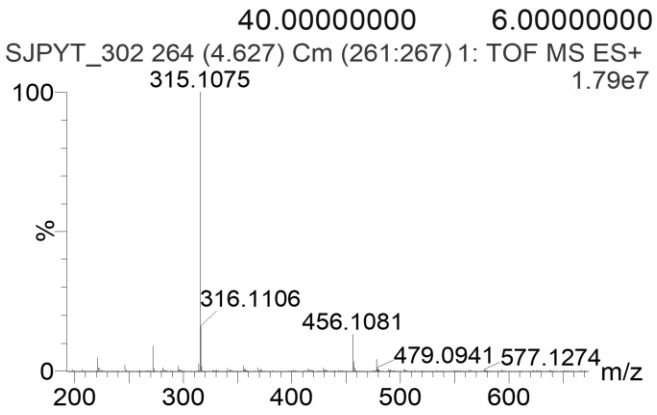

Figure S7. HRMS of SJPYT-302.

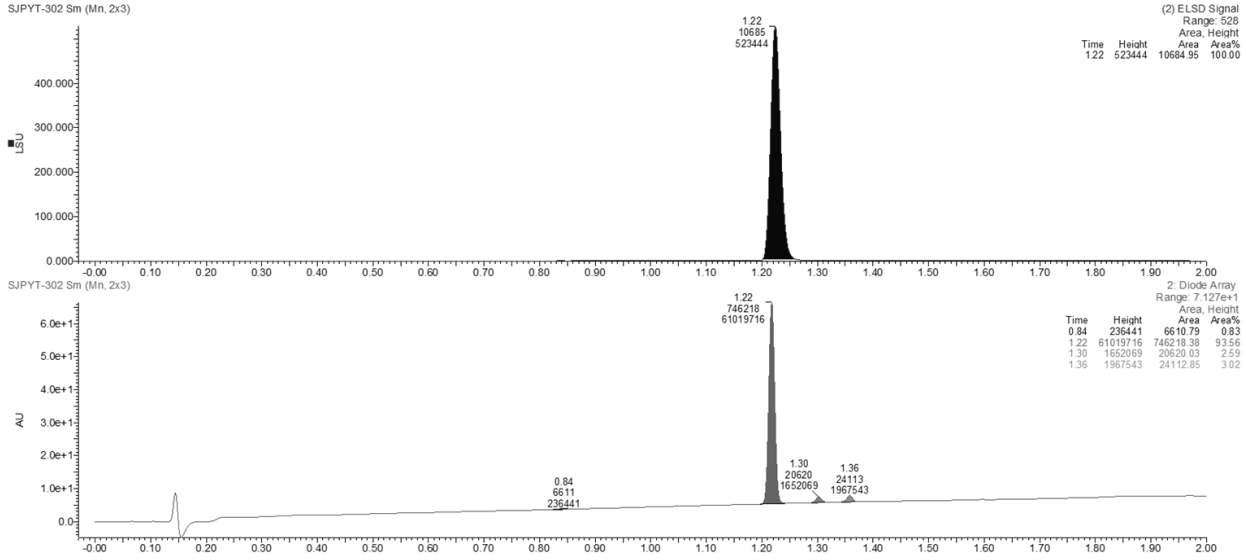

Figure S8. HPLC of SJPYT-302.

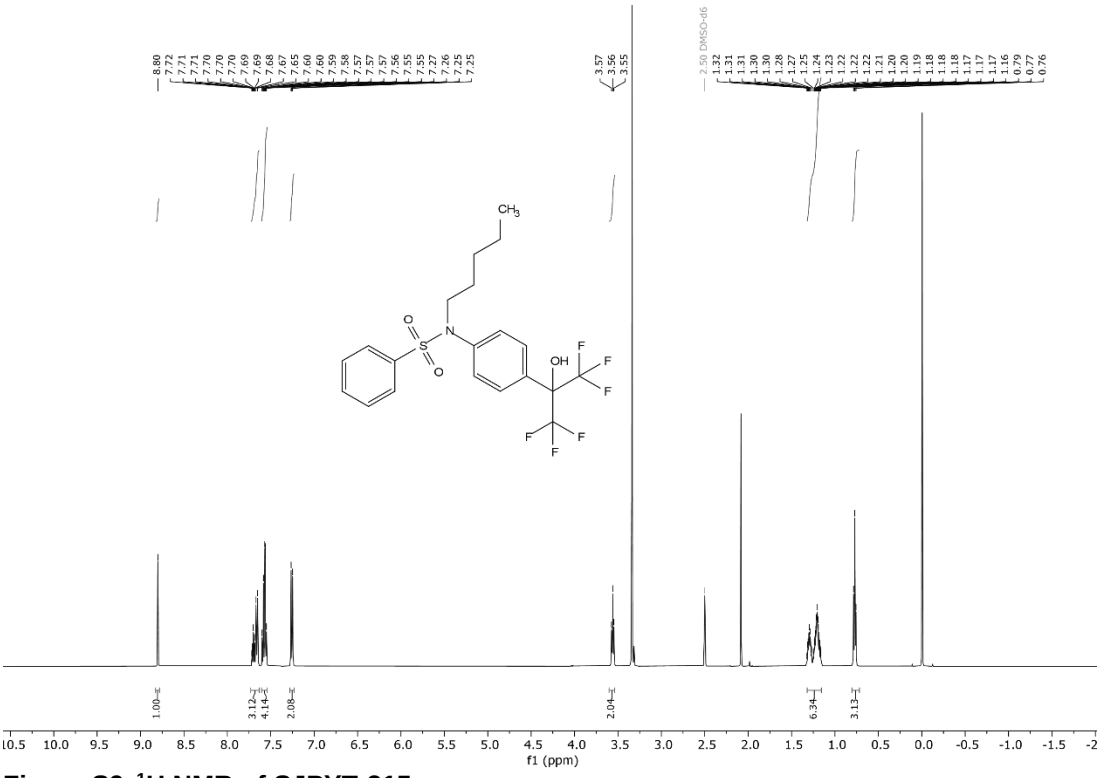

Figure S9. ^{1}H NMR of SJPYT-315.

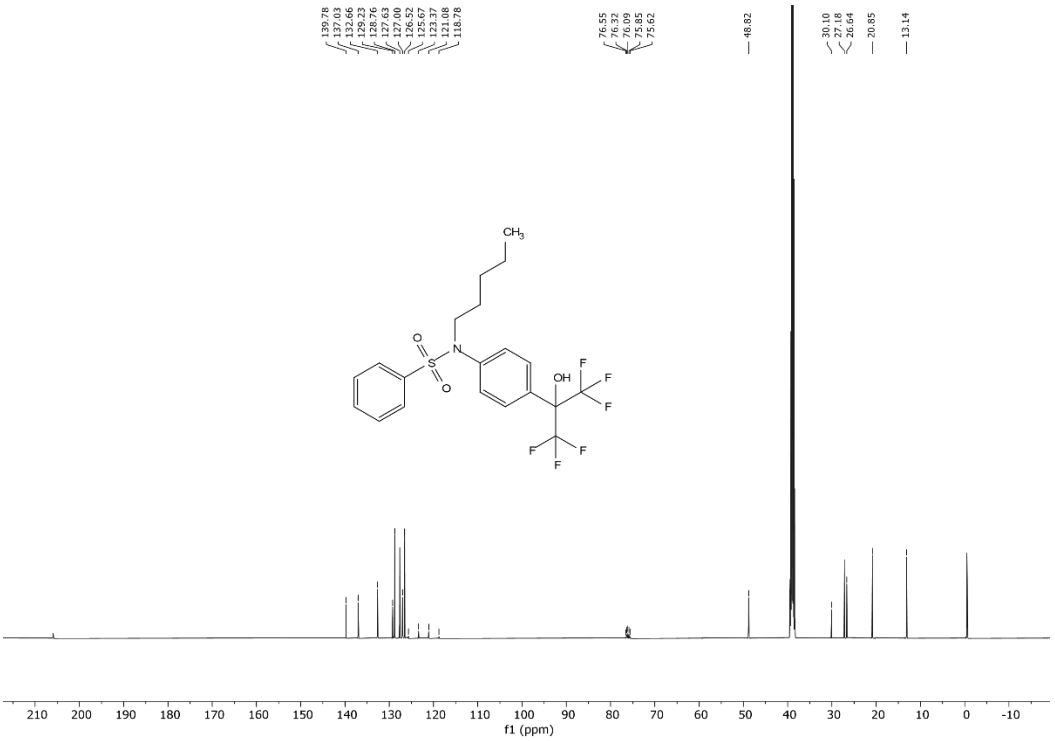

Figure S10. ^{13}C NMR of SJPYT-315.

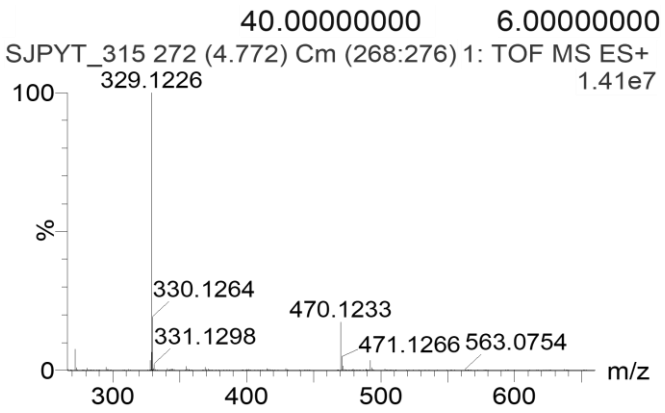

Figure S11. HRMS of SJPYT-315.

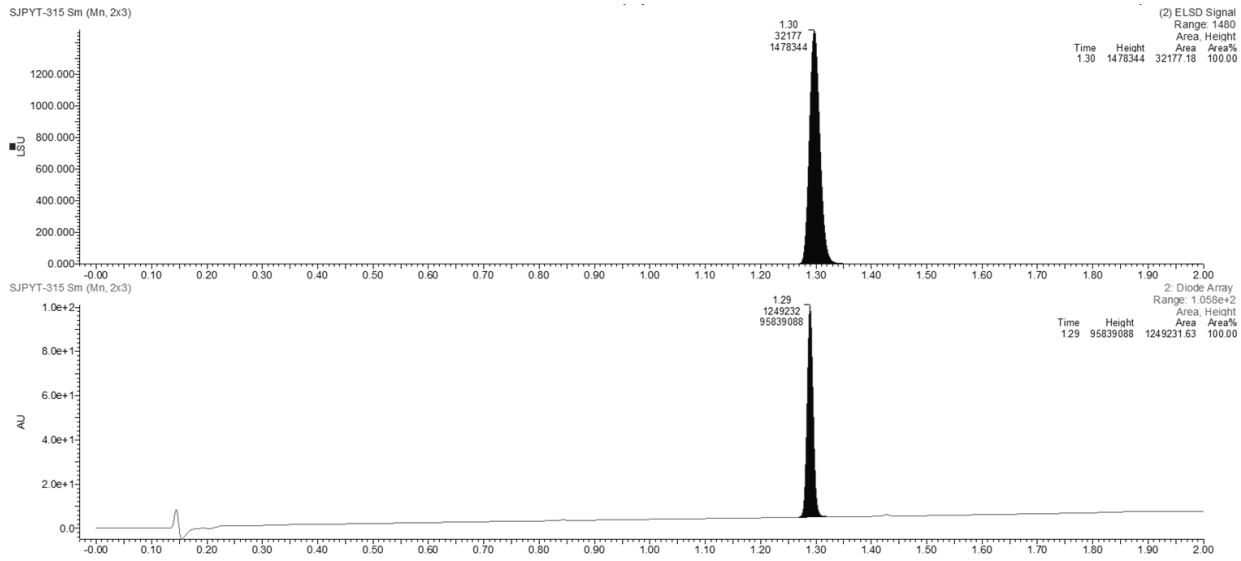

Figure S12. HPLC of SJPYT-315.

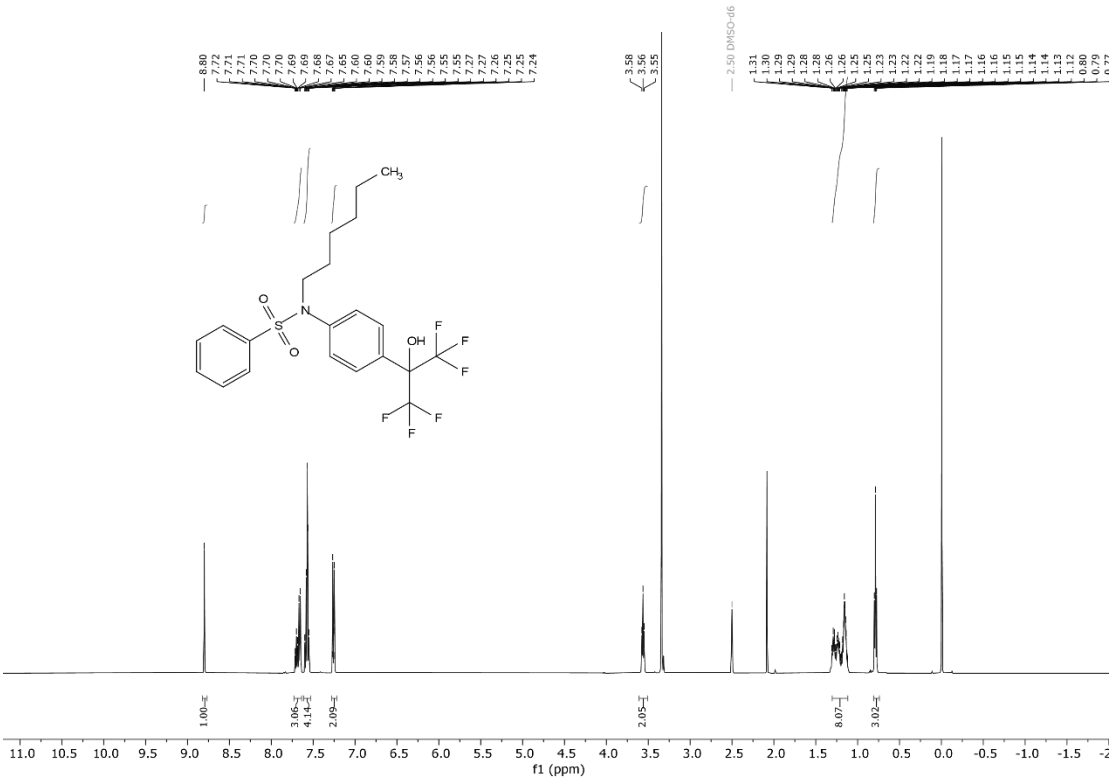

Figure S13. ^{1}H NMR of SJPYT-316.

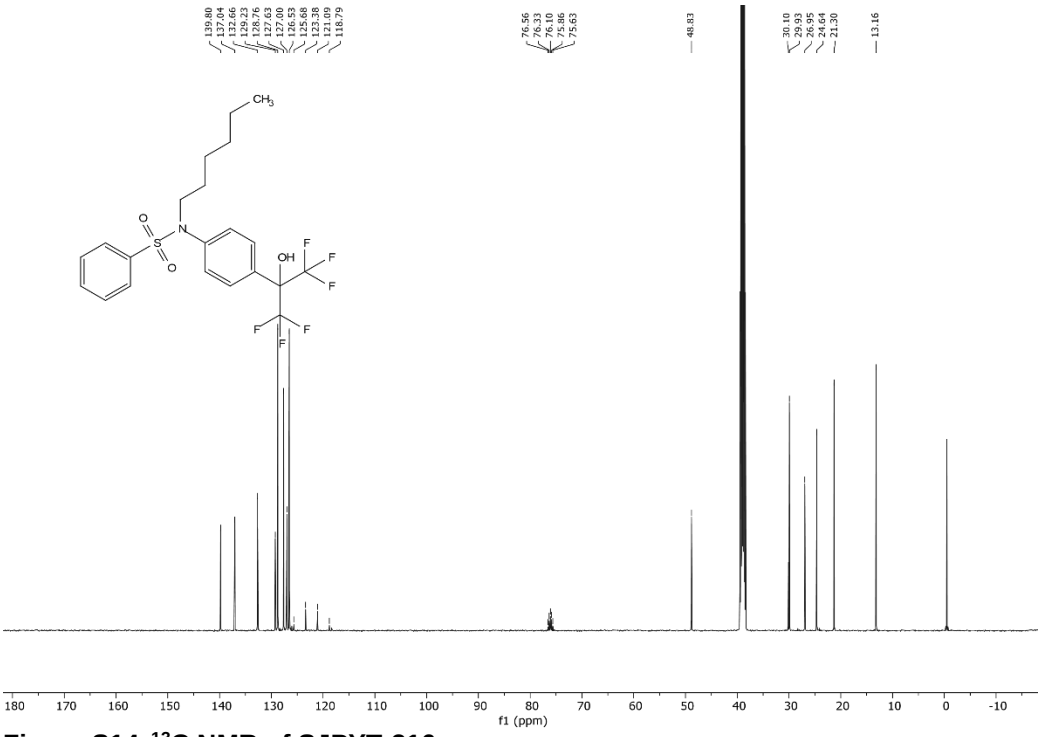

Figure S14. ^{13}C NMR of SJPYT-316.

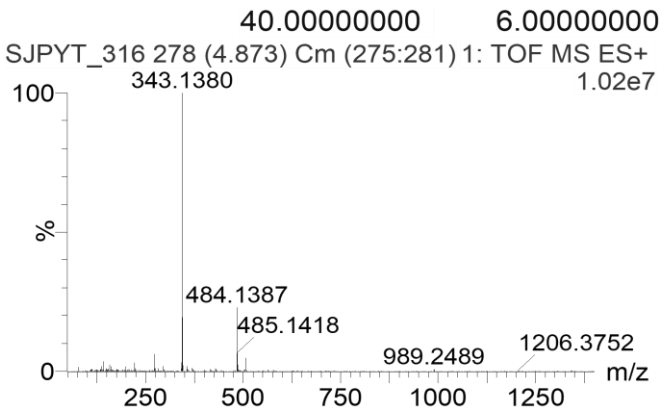

Figure S15. HRMS of SJPYT-316.

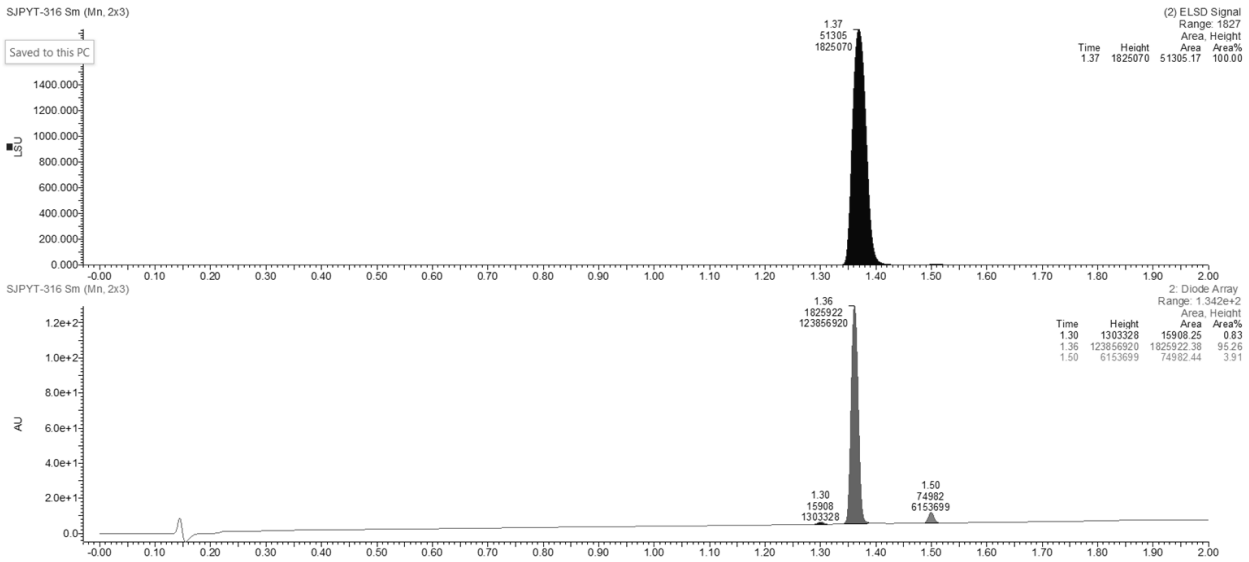

Figure S16. HPLC of SJPYT-316.

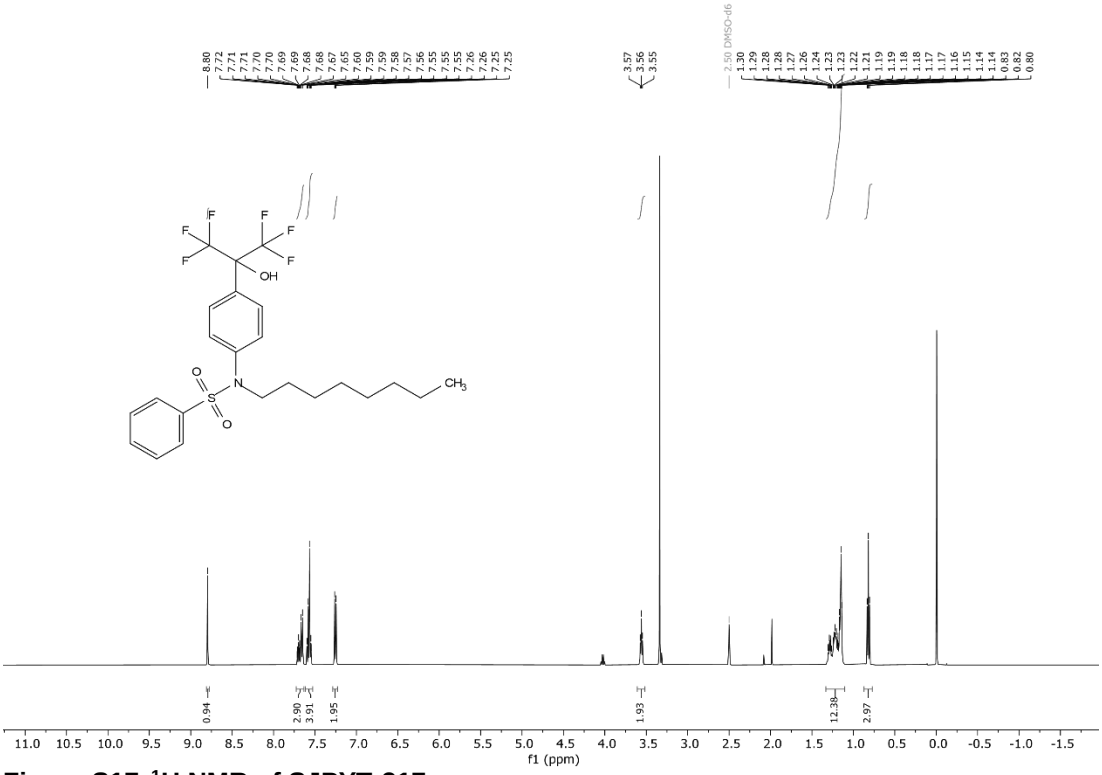

Figure S17. ^{1}H NMR of SJPYT-317.

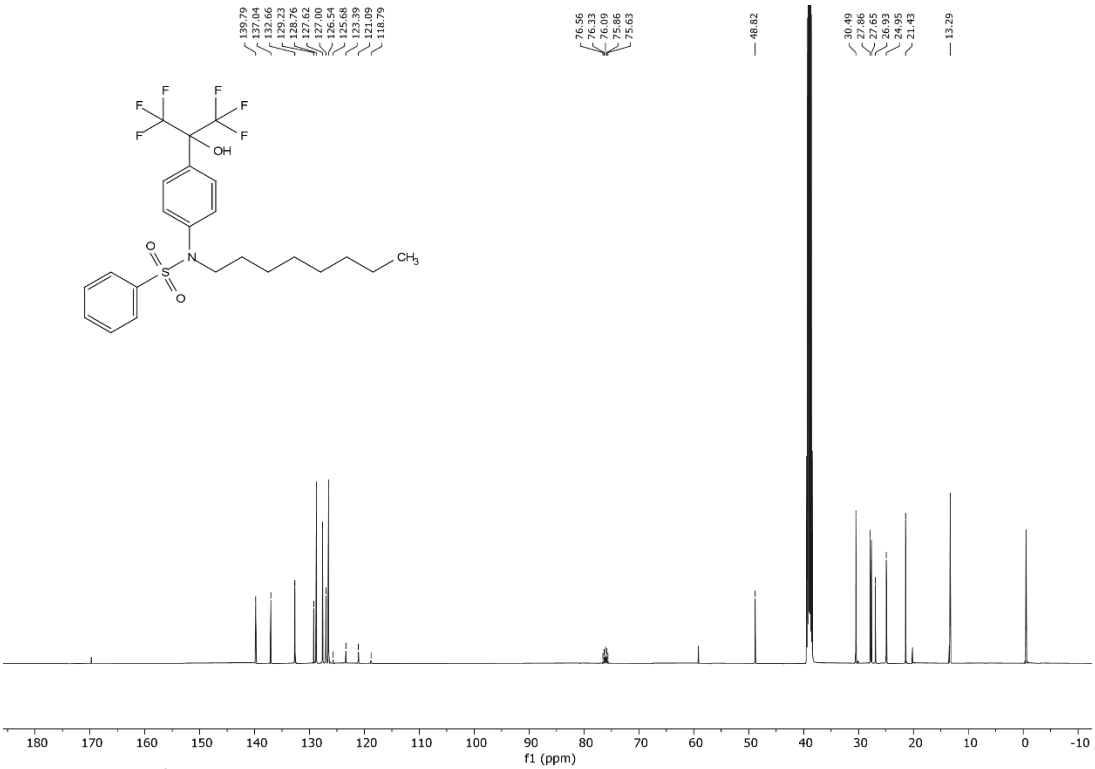

Figure S18. ^{13}C NMR of SJPYT-317.

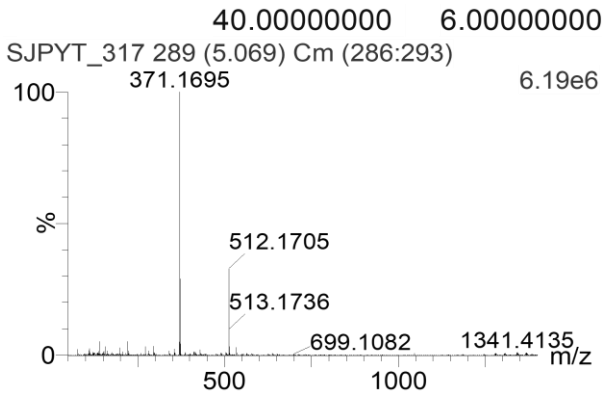

Figure S19. HRMS of SJPYT-317.

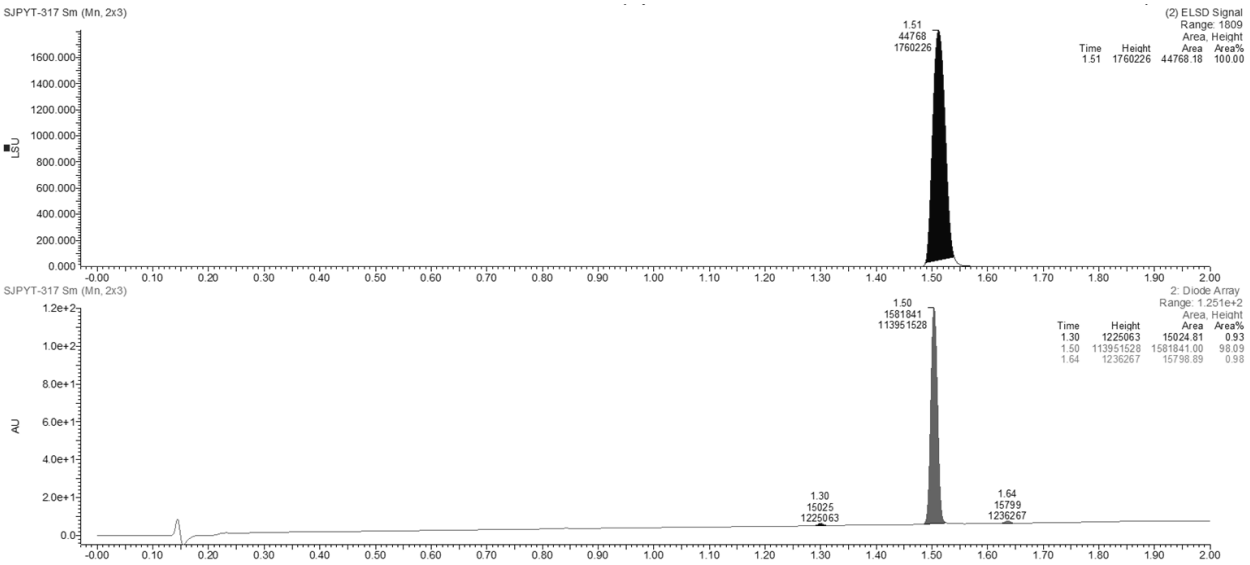

Figure S20. HPLC of SJPYT-317.

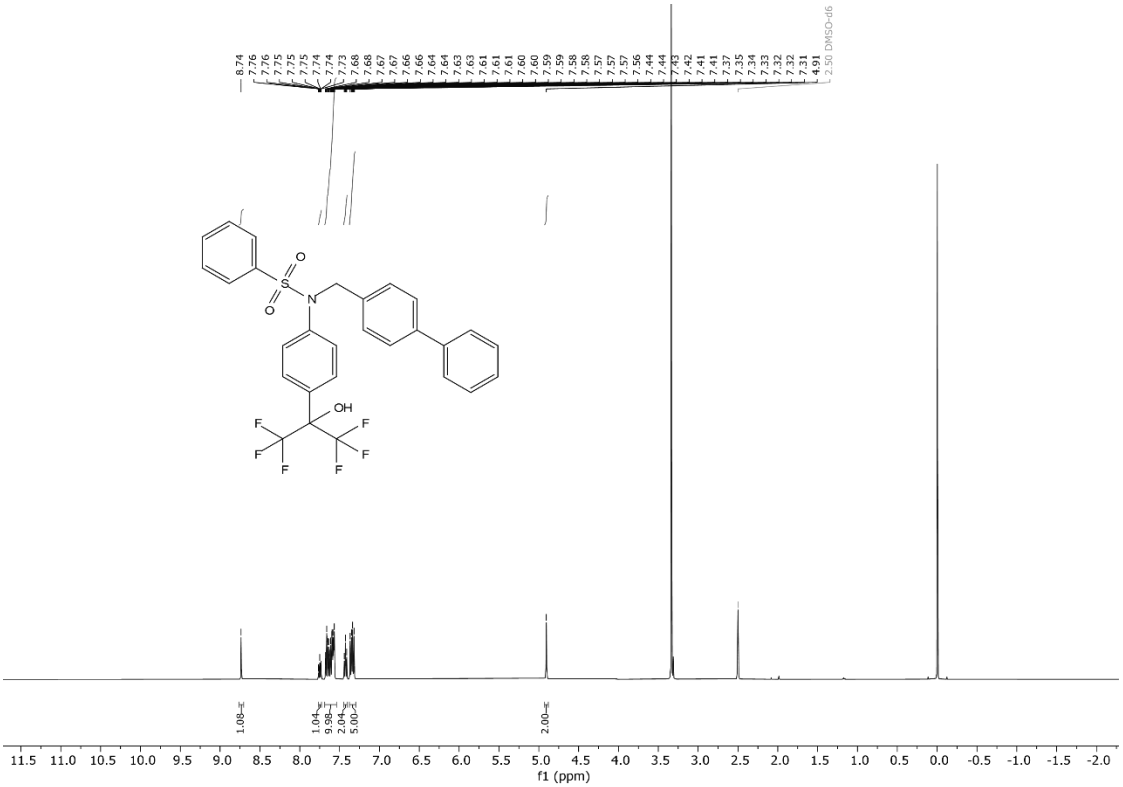

Figure S21. ^{1}H NMR of SJPYT-319.

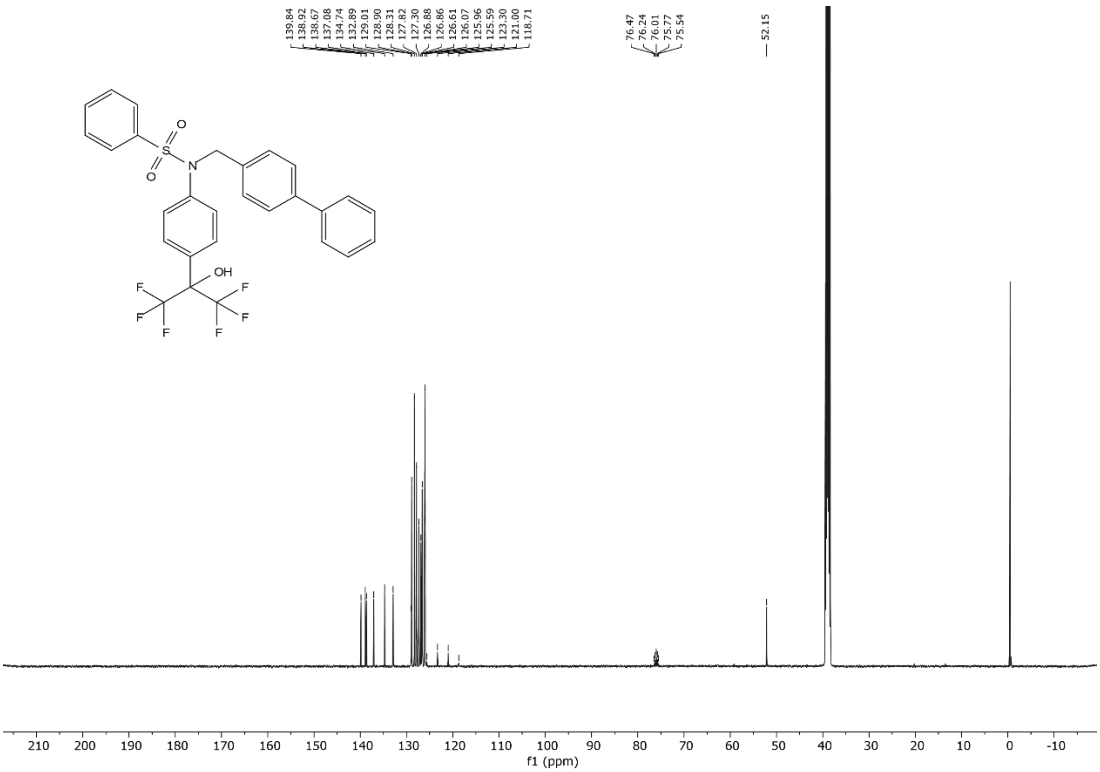

Figure S22. ^{13}C NMR of SJPYT-319.

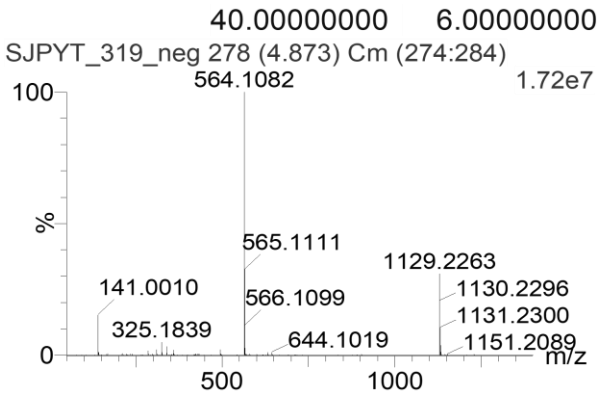

Figure S23. HRMS of SJPYT-319.

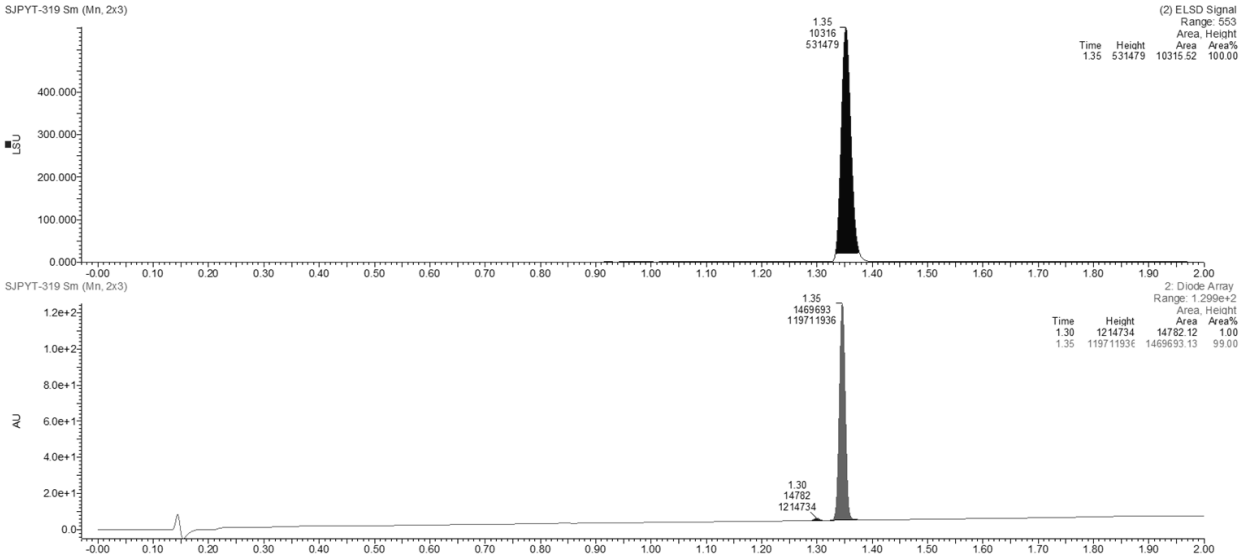

Figure S24. HPLC of SJPYT-319.

SI References

1. B. P. Fauber *et al.*, Structure-based design of substituted hexafluoroisopropanol-arylsulfonamides as modulators of RORc. *Bioorg Med Chem Lett* **23**, 6604-6609 (2013).